CHAPTER THREE

Single-Molecule Optical-Trapping Techniques to Study Molecular Mechanisms of a Replisome

B. Sun*, M.D. Wang†,‡,1

*School of Life Science and Technology, ShanghaiTech University, Shanghai, PR China
†Laboratory of Atomic and Solid State Physics, Cornell University, Ithaca, NY, United States
‡Howard Hughes Medical Institute, Cornell University, Ithaca, NY, United States
1Corresponding author: e-mail address: mwang@physics.cornell.edu

Contents

1. Introduction 56
2. Instrument Design, Experimental Configuration, and Sample Preparation 57
   2.1 Layout of an Optical-Trapping Apparatus 57
   2.2 Experimental Configuration 59
   2.3 Preparation of Experimental Sample Chambers 60
3. Molecular Mechanisms of Individual Proteins in the Replisome Revealed by Optical-Trapping Techniques 61
   3.1 DNA Template Design and Construction 61
   3.2 Helicase-Unwinding Assay 64
   3.3 Helicase Translocation Assay 66
   3.4 Polymerase Strand Displacement Assay 67
4. Single-Molecule Studies of the Response of a Replisome to DNA Damage 69
   4.1 DNA Template Design and Construction 70
   4.2 Response of Individual Proteins to DNA Damage: Helicase-Unwinding Assay and Polymerase Strand Displacement Assay. 72
   4.3 Response of a Replisome to DNA Damage: Leading-Strand Replication Assay 74
5. Data Analysis 74
   5.1 DNA Elastic Parameter Determination 74
   5.2 DNA Extension Conversion to Number of Base Pairs 76
   5.3 Helicase Slippage Determination and Processivity Measurements 77
   5.4 Unwinding Rate and Replication Rate Measurements and Comparison 77
   5.5 Fate of a Replisome Encountering DNA Damage 78
6. Unique Features of the Bacteriophage T7 Replisome Revealed by Single-Molecule Optical-Trapping Techniques 79
   6.1 Helicase Slippage and Subunit Coordination 79
   6.2 Inherent Tolerance of the T7 Replisome to DNA Damage 80

Methods in Enzymology, Volume 582
ISSN 0076-6879
http://dx.doi.org/10.1016/bs.mie.2016.08.001

7. Conclusions 81
Acknowledgments 81
References 81

Abstract

The replisome is a multiprotein molecular machinery responsible for the replication of DNA. It is composed of several specialized proteins each with dedicated enzymatic activities, and in particular, helicase unwinds double-stranded DNA and DNA polymerase catalyzes the synthesis of DNA. Understanding how a replisome functions in the process of DNA replication requires methods to dissect the mechanisms of individual proteins and of multiproteins acting in concert. Single-molecule optical-trapping techniques have proved to be a powerful approach, offering the unique ability to observe and manipulate biomolecules at the single-molecule level and providing insights into the mechanisms of molecular motors and their interactions and coordination in a complex. Here, we describe a practical guide to applying these techniques to study the dynamics of individual proteins in the bacteriophage T7 replisome, as well as the coordination among them. We also summarize major findings from these studies, including nucleotide-specific helicase slippage and new lesion bypass pathway in T7 replication.

1. INTRODUCTION

DNA replication is carried out by the replisome, a large protein complex that includes DNA helicase, DNA polymerase (DNAP), and other proteins (Benkovic, Valentine, & Salinas, 2001). The bacteriophage T7 replisome has been identified to be a simple and efficient model system for the study of DNA replication (Hamdan & Richardson, 2009), as only four proteins are required for basic phage replication, yet it mimics more complex systems. Briefly, T7 DNAP, a 1:1 complex of gene 5 protein (gp5) and its processivity factor *Escherichia coli* thioredoxin (trx), is responsible for nucleotide polymerization (Tabor, Huber, & Richardson, 1987). The protein product of T7 gene 4 (gp4) provides helicase and primase activities (Matson, Tabor, & Richardson, 1983). The helicase activity, required for unwinding the parental DNA strand, resides in the C-terminal half of the protein, while the primase activity, required to initiate lagging-strand DNA synthesis by synthesizing RNA primers, is located in the N-terminal of the protein. T7 helicase is a hexameric motor and couples the hydrolysis of nucleoside triphosphate to translocate along single-stranded DNA (ssDNA) and unwind double-stranded DNA (dsDNA) (Donmez & Patel, 2008; Singleton, Dillingham, & Wigley, 2007). Finally, the product of gene 2.5 of bacteriophage T7 (gp2.5), a single-stranded DNA-binding (SSB) protein,

coats ssDNA to remove its secondary structure (Kim & Richardson, 1993). Although tremendous advances are being made in our understanding of the structures and functions of these proteins (Hamdan & Richardson, 2009), their dynamic and mechanistic properties are not fully understood. For example, how do different subunits of the hexameric helicase coordinate their chemical and mechanical activities to translocate along ssDNA? How does the helicase coordinate with DNAP during replication? How does DNAP deal with DNA lesions in a template strand?

These questions are well suited to be investigated by optical trapping, a powerful single-molecule technique that offers the unique ability to observe and manipulate biomolecules at the single-molecule level. By directly revealing biomolecular dynamic behaviors in real time, this approach can provide essential information and complement ensemble studies in understanding various biological systems (Moffitt, Chemla, Smith, & Bustamante, 2008; Sun & Wang, 2016). Optical trapping provides flexible control of both force and extension of the substrate, enabling rapid switching between different modes of operation. In this chapter, using the bacteriophage T7 replisome as an example, we detail experimental procedures utilizing optical-trapping techniques to study molecular mechanisms of individual proteins in the replisome. In addition, we also provide a practical guide to dissecting the response of the T7 replisome to DNA damage.

2. INSTRUMENT DESIGN, EXPERIMENTAL CONFIGURATION, AND SAMPLE PREPARATION

2.1 Layout of an Optical-Trapping Apparatus

In general, an optical trap is generated by using a high-numerical aperture microscope objective to focus tightly a laser beam to a diffraction limited beam waist. The gradient of the intensity provides the trapping force, which can be used to manipulate a trapped dielectric microsphere. Here, we use a single-beam optical-trapping instrument containing the minimal set of optical components required for the operation of a high-precision instrument of its kind (Fig. 1) (Brower-Toland & Wang, 2004; Koch, Shundrovsky, Jantzen, & Wang, 2002; Li & Wang, 2012). In brief, a 1064-nm Gaussian laser (J20I-8S-12K-NSI, Spectra-Physics Lasers, Inc., Mountain View, CA) is coupled to a single-mode fiber (PMJ-A3A, 3AF-1064-6/125-sAS-12-1, Oz Optics, Carp, ON). After collimation, the beam is expanded by a telescope lens pair and then focused onto the back focal plane of a 100×, 1.4 NA oil immersion microscope objective (Plan Apo 100×/1.40 Oil IR, Nikon, Melville, NY). An acousto-optic deflector (AOD) (AOBD

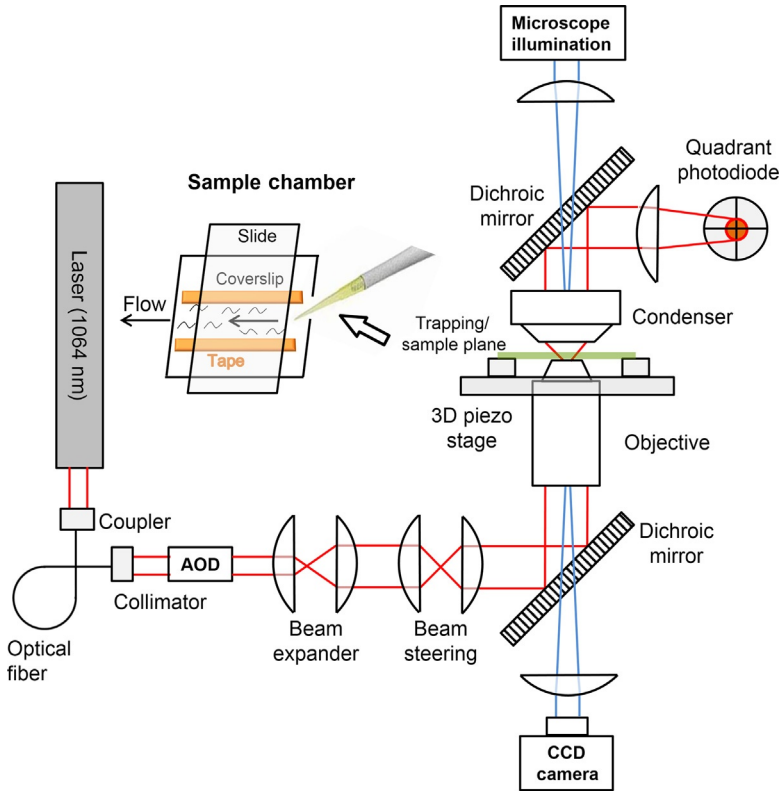

Fig. 1 Layout of the optical-trapping apparatus and a schematic of the sample chamber. See text for a detailed description of the setup.

N45035-3-6.5DEG-1.06, NEOS Technologies, Inc., Melbourne, FL) is placed between the laser aperture and the beam expander to adjust the laser intensity. The beam is then introduced into a modified Eclipse Nikon TE200 inverted microscope's imaging path (Nikon, Melville, NY). Upon beam collection by a condenser, the laser beam is imaged onto a quadrant photodiode (S5981, Hamamatsu, Bridgewater, NJ), at which a deflection voltage signal reflects a displacement of a trapped microsphere. A high-precision 3D piezoelectric stage (Nano-PDQ350HS, Mad City Labs, Madison, WI) is used to position a sample chamber. Analog voltage signals generated by the position detector and piezo stage position sensor are antialias filtered at 5 kHz (part number 3384, Krohn-Hite, Avon, MA) and digitized at 7–13 kHz, using a multiplexed analog-to-digital conversion PCIe board (NI PCIe-6259, National Instruments Corporation, Austin, TX). The instrument

calibration methods and experimental control modes, such as force clamp and velocity clamp, were described in previous publications (Li & Wang, 2012).

2.2 Experimental Configuration

To mimic a DNA replication fork, we typically start an experiment with a DNA template containing a fork junction initially or after mechanically unzipping of a dsDNA (see Sections 3.1 and 4.1) (Johnson, Bai, Smith, Patel, & Wang, 2007; Sun et al., 2011, 2015). As shown in Fig. 2, the ends of the leading and lagging strands are differentially labeled, generally by digoxigenin and biotin. One strand is attached to a trapped 500 nm microsphere via a biotin/streptavidin connection, and the other strand is anchored to a microscope coverslip surface via a digoxigenin/antidigoxigenin connection. The microsphere is held in a feedback-enhanced optical trap so that both its position and force can be measured. Experiments are typically conducted under a constant force where the coverslip position is modulated to maintain a constant force on the trapped microsphere. Helicase unwinding, DNA synthesis or degradation, and helicase-unwinding coupled DNA synthesis are reflected as a change in the DNA length between the microsphere and the anchor point on the coverslip.

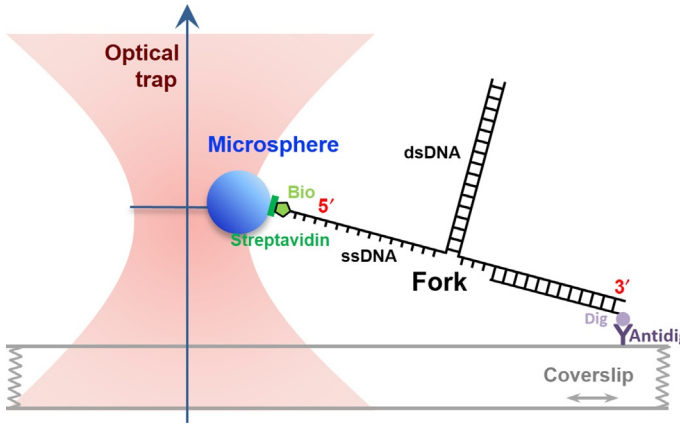

Fig. 2 Experimental configuration for the studies of a replisome. An optical trap is used to exert a force on a trapped microsphere and monitor extension change resulting from the activities of motor proteins at the fork. The extremities of a DNA template are attached to the coverslip and microsphere via digoxigenin/antidigoxigenin and biotin/streptavidin connections, respectively.

2.3 Preparation of Experimental Sample Chambers

Prior to mounting onto an optical setup, sample chambers are prepared at room temperature in a humid chamber to minimize buffer evaporation (Johnson et al., 2007; Li & Wang, 2012). Briefly, two thin pieces of double-stick transparent tape (~0.1 mm thick) are first applied in parallel with ~5 mm separation to a coverslip (24 mm × 40 mm × 0.15 mm). Then, a glass slide (25 mm × 76 mm × 1.2 mm) is perpendicularly placed on top of the coverslip, creating a ~15 μL volume channel bordered by the two strips of tape (Fig. 1). To immobilize individual DNA tethers in the sample chamber, different solutions are sequentially flowed into the chamber. Polyclonal sheep antidigoxigenin (Roche Applied Sciences), diluted in PBS buffer, is used first to coat the coverslip, followed by a blocking buffer (a typical blocking agent is casein sodium salt from bovine milk, Sigma-Aldrich Co.) to prevent unwanted protein and DNA attachment to the surface. After thoroughly washing the chamber by flowing in excess volumes of experiment-specific reaction buffer (see Sections 3.2 and 4.3 for details), proper concentration of DNA and microspheres are sequentially flowed into the chamber to form DNA tethers. The detailed procedure is:

(1) Flow in 1 volume (~15 μL) of antidigoxigenin solution (20 ng/μL) in PBS and incubate for 5 min.

(2) Wash with 5 volumes of blocking buffer (5 mg/mL casein sodium slat from bovine milk in reaction buffer) and incubate with residual blocker for 5 min.

(3) Wash with 5 volumes of reaction buffer and sequentially flow in 1 volume of diluted DNA template in the sample buffer. Incubate for 10 min.

(4) Wash with 5 volumes of sample buffer and sequentially flow in 1 volume of streptavidin-coated polystyrene microspheres (5 p*M* in blocking buffer). Incubate for 10 min.

(5) Wash with 10 volumes of reaction buffer with one or more replicative proteins of interest and Mg^{2+} at proper concentrations and place the sample chamber on the optical setup for experiments.

It is worth noting here that DNA samples need to be diluted to a proper concentration to achieve an optimal surface tether density under single-molecule conditions. Low DNA concentrations will cause low tether density, making it difficult to spot a suitable tether in the chamber. Conversely, high DNA concentrations will lead to multiple DNA molecules attaching to one microsphere. The optimal concentration of DNA depends on the

specific DNA template design and construction. In practice, tens to hundreds of pico molar of DNA sample is needed to achieve an acceptable tether density.

3. MOLECULAR MECHANISMS OF INDIVIDUAL PROTEINS IN THE REPLISOME REVEALED BY OPTICAL-TRAPPING TECHNIQUES

3.1 DNA Template Design and Construction

Here, we detail the construction of DNA templates that can be used with optical-trapping system for the studies of individual proteins in the replisome (helicase or polymerase). A template generally consists of two segments: an anchoring segment and an unwinding segment, separated by a nick, which allows the DNA to be mechanically unwound (unzipped) (Fig. 3D) (Dechassa et al., 2011; Hall et al., 2009; Jiang et al., 2005; Jin et al., 2010;

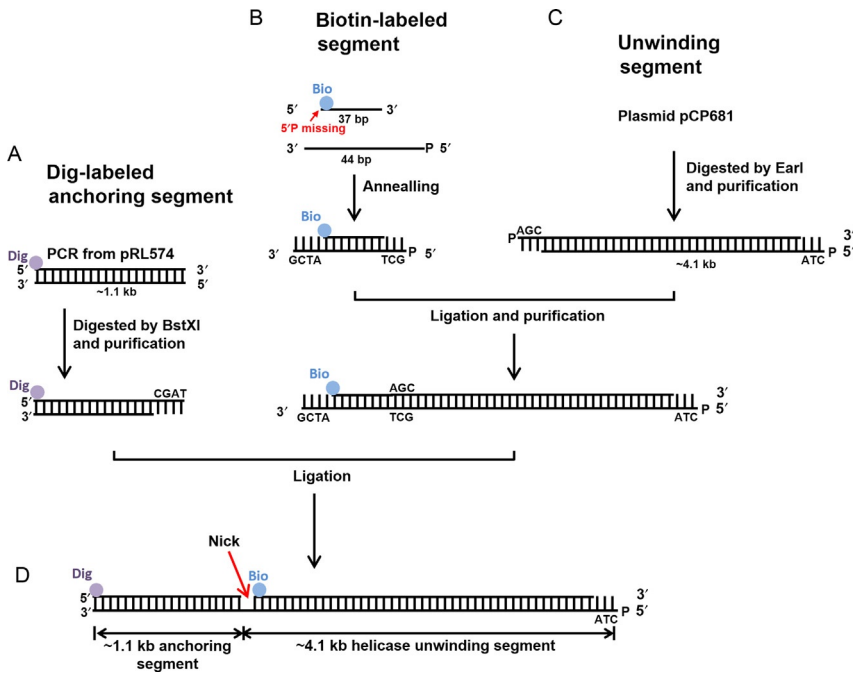

Fig. 3 Unwinding template construction. A DNA template for the studies of individual proteins in the replisome is a product of ligation (D) of digoxigenin-labeled anchoring segment (A) and biotin-labeled unwinding segment. The unwinding segment consists of a biotin-labeled segment (B) and experiment-specific unwinding segment (C). See text for a detailed description of the experimental procedures.

Koch & Wang, 2003; Koch et al., 2002; Li et al., 2015; Shundrovsky, Smith, Lis, Peterson, & Wang, 2006; Sun et al., 2011). The end of the anchoring segment is labeled by digoxigenin for attachment to the coverslip, and a biotin in the unwinding segment near the nick may be attached to a streptavidin-coated microsphere. By moving the coverslip away from the trapped microsphere to unzip the unwinding segment mechanically, a replication fork will be generated, allowing helicase loading/unwinding or polymerase synthesis.

To provide sufficient separation between the anchor point and the unwinding segment while minimizing the Brownian motion of the trapped microsphere, the anchoring segment with an end-labeled digoxigenin tag is generally 1–2 kbp long. The unwinding segment is made of a biotin tagged segment followed by an experiment-specific target sequence. The length of the unwinding segment can vary from 800 to 4000 bp. As an example, we provide later a detailed protocol for constructing a 5.2-kbp DNA template containing a 1.1-kbp anchoring segment and a 4.1-kbp unwinding segment (Johnson et al., 2007). The unwinding segment is derived from 17 pseudo-repeats (or 17mer) of the 5S rRNA sequence, consisting of three five-repeats (or 5mer) of 207 bp, joined together by a 224 bp linking region. See later and Fig. 3 for detailed procedure.

Anchoring segment preparation (Fig. 3A)

(1) PCR amplify the anchoring segment from plasmid pRL574 (Koch et al., 2002). The forward primer (all primers and oligonucleotides were purchased from Integrated DNA Technologies and are listed in Table 1, unless specified otherwise) contains a 5′-digoxigenin label, designed to be 1.1 kbp away from the single BstXI (New England Biolabs, NEB) cutting site located on the plasmid.

(2) BstXI digest the PCR product to generate a 3′-overhang for ligation of the unzipping segment.

Unwinding segment preparation

(3) Anneal two oligonucleotides to form a short biotin segment (Fig. 3B). One of the oligonucleotides is 5′-biotin labeled and lacks a phosphate for the generation of a nick. After annealing, two overhangs are generated for the ligation to the anchoring segment and 17mer segment.

(4) The 17mer segment is a digestion product from plasmid pCP681 (Fig. 3C). After cutting with EarI (NEB), the desired segment is purified using an agarose gel purification kit (Zymo Research).

Table 1 Primers and Oligonucleotides Used for DNA Templates Construction

5.2 kbp nicked DNA template	Anchoring segment	Forward primer	5′-/dig/ GTT GTA AAA CGA CGG CCA GTG AAT
		Reverse primer	5′-CCG TGA TCC AGA TCG TTG GTG AAC
	Biotin segment	Biotin oligo	5′-/bio/ GAG CGG ATT ACT ATA CTA CAT TAG AAT TCG GAC
		Complementary oligo	5′-/phos/ GCT GTC TGA ATT CTA ATG TAG TAT AGT AAT CCG CTC ATC G
Y-shaped lesion-containing DNA template	Arm 1	Forward primer	5′-/dig/ GTT GTA AAA CGA CGG CCA GTG AAT
		Revise primer	5′-GAT CCA GAT CGT TGG TGA AC
	Arm 2	Forward primer	5′-/bio/ GAT GCT TTT CTG TGA CTG GTG AG
		Reverse primer	5′-ACG GTT ACC AGC CTA GCC GGG TCC TCA
	Adapters	Adapter 1	5′-/phos/ GCA GTA CCG AGC TCA TCC AAT TCT ACA TGC CGC
		Adapter 2	5′-/phos/ GCC TTG CAC GTG ATT ACG AGA TAT CGA TGA TTG CGG CGG CAT GTA GAA TTG GAT GAG CTC GGT ACT GCA TCG
		Adapter 3	5′-/phos/ GTA ACC TGT ACA GTG TAT AGA ATG ACG TAA CGC GCA ATC ATC GAT ATC TCG TAA TCA CGT GCA AGG CCT A
	Upstream segment	Forward primer	5′-CGC AGC TAC TGA GCC AGT CTG GTC ACA AGC G
		Reverse primer	5′-GAT GGT CTC ACG GTT GGC GTC ATC GTG T

Continued

Table 1 Primers and Oligonucleotides Used for DNA Templates Construction—cont'd

Lesion segment	Lesion oligo	5′-/phos/ GGT GTC ACC AGC AGG CCG ATT GGG TT (CPD lesion) G GGT ATT CGC CGT GTC CCT CTC GAT GGC TGT AAG TAT CCT ATA GG
	Complementary oligo	5′-/phos/ ACC GCC TAT AGG ATA CTT ACA GCC ATC GAG AGG GAC ACG GCG AAT ACC CAAC CCA ATC GGC CTG CTG GTG ACA CCC GAT
Downstream segment	Forward primer	5′-TCA CCA ACG ATC TGG ATC ACG
	Revise primer	5′-CGG TTG GCG TCA TCG TGT

(5) Ligate the 17mer segment with the biotin segment (1:10 molar ratio) at 16°C for 4 h using T4 ligase (NEB) to form the unwinding segment. Purify the ligated products using agarose gel purification to remove excess biotin segment.

Anchoring segment and unwinding segment ligation

(6) The final product is produced by ligating the anchoring segment and the unwinding segment using T4 ligase (in a 1:1 molar ratio) (Fig. 3D). Overnight ligation is normally necessary to maximize the ligation yield. A complete template is stable for a few days at 4°C.

An advantage of this DNA template design is that, in the experiments, the DNA that has failed the final ligation step is automatically excluded, as the biotin for microsphere attachment is located on the unwinding segment such that no tether can be formed without this segment.

3.2 Helicase-Unwinding Assay

Here, we detail the experimental procedures, using the aforementioned DNA template, to study T7 helicase unwinding (Fig. 4A) (Johnson et al., 2007; Sun et al., 2011).

T7 helicase consists of homologous monomers that form a ring-shaped hexamer (Donmez & Patel, 2006). It binds one strand of dsDNA within its central channel, while excluding the complementary strand

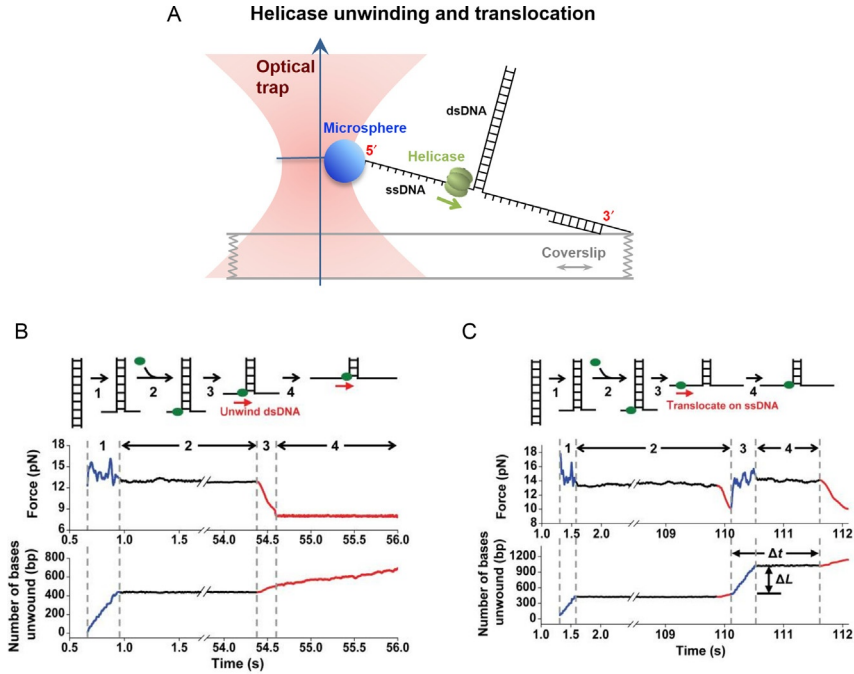

Fig. 4 Helicase unwinding and translocation assays. (A) Experimental configuration for helicase unwinding and translocations assays by a single T7 helicase. (B) and (C) correspond to helicase unwinding and translocation assays, respectively, in 2 m*M* dTTP. See text for a detailed description of the experimental procedures. *Adapted from Johnson, D. S., Bai, L., Smith, B. Y., Patel, S. S., & Wang, M. D. (2007). Single-molecule studies reveal dynamics of DNA unwinding by the ring-shaped T7 helicase.* Cell, 129, *1299–1309, with permission from the publisher.*

(Ahnert & Patel, 1997). First, prepare T7 helicase by diluting helicase in its reaction buffer (50 m*M* NaCl, 3 m*M* EDTA, and 0.02% Tween-20 in 20 m*M* Tris–HCl, pH 7.5), followed by incubating 2 μ*M* helicase, in the presence of 2 m*M* NTP and 3 m*M* EDTA, for 20 min to form a hexamer in which form T7 helicase is able to load onto ssDNA. Prior to flowing it into the sample chamber, the solution is diluted to a proper concentration (depending on the type of nucleotide used, see later), in 2 m*M* NTP, 3 m*M* EDTA, and 7 m*M* $MgCl_2$ (Johnson et al., 2007; Patel et al., 2011; Sun et al., 2011). A detailed procedure to detect helicase unwinding is provided as follows (Fig. 4B):

(1) Mechanically unzipping to generate ssDNA. A tethered microsphere is used to stretch out the DNA under a "velocity clamp" mode, where the coverslip is moved away from the trapped microsphere at constant rate.

The position of the microsphere in the trap is kept constant by modulating the light intensity (trap stiffness) of the trapping laser. In this mode, the dsDNA in the unwinding segment is mechanically unzipped to generate ssDNA.

(2) Helicase loading. After ~400 bp of dsDNA is mechanically unzipped, the setup is switched to a "hold" mode, in which the piezo stage and the light intensity are kept constant. Freely diffusing helicase can load onto the ssDNA, translocate from 5′ to 3′, and subsequently unwind the remaining dsDNA, resulting in an increase of ssDNA length and, thereby, a decrease in its tension.

(3) Helicase unwinding under constant force. The "hold" mode is exited to a "force clamp" mode after the force becomes lower than a preset value which is below that to unzip the DNA mechanically. In the "force clamp" mode, the force on the DNA tether is kept constant by adjusting both the position of the piezo stage and the light intensity. Therefore, the kinetics of helicase unwinding is measured by following the fork junction motion in real time.

To ensure there is a single T7 helicase on the template, helicase concentration needs to be low enough so that the average helicase arrival time at the fork junction is significantly longer than the typical measurement time (Johnson et al., 2007). In the presence of dTTP, we typically used 0.3 n*M* hexameric helicase (~2 n*M* monomer) as the final concentration in our experiments. ATP binds to T7 helicase with a weaker affinity than dTTP (Hingorani & Patel, 1996; Lee & Richardson, 2010; Matson & Richardson, 1983), and thus a higher concentration of T7 helicase (e.g., 10 n*M* hexameric helicase) is recommended in the presence of ATP. Helicase slippage was also observed in this condition (see Section 6.1). For the experiments in which both nucleotides are present, 1 n*M* hexameric helicase is an appropriate concentration to achieve single helicase activity.

3.3 Helicase Translocation Assay

The helicase translocation assay aims to investigate the ssDNA translocation rate of helicase on long stretches of ssDNA (Johnson et al., 2007). We have used the unzipping fork to mark the initial and final positions and times of the helicase translocation. The helicase's arrival at a fork and its subsequent unwinding of the fork leads to a force drop, which marks the initial position and start time of the helicase translocation. Immediately following this detection, a region of downstream ssDNA is rapidly generated via

mechanically unzipping. Helicase then translocates on this newly available ssDNA until it catches up with, and unwinds, the downstream fork, leading to another force drop which marks the final position and time for the helicase translocation. The ssDNA translocation rate is obtained from the distance that the helicase travels over the time the helicase takes to translocate this distance. The detailed procedure is listed below (Fig. 4C):

(1) Mechanically unzipping to generate ssDNA. Using a "velocity clamp" mode, dsDNA in the unwinding segment is mechanically unzipped to provide a segment of ssDNA.

(2) Detection of helicase loading. The setup is switched to a "hold" mode, and the DNA extension is maintained until the force drops below a threshold indicating helicase unwinding of the DNA fork.

(3) Mechanically unzipping to generate more ssDNA. Mechanically unwind about 600 bp to generate a new ssDNA region for helicase translocation. Transition to a "hold" mode again.

(4) Detection of helicase arrival at the fork. Maintain the new DNA fork position until force drops again, indicating that the helicase has caught up with the fork.

Using this method, it should be noted that the translocation rate on ssDNA is obtained under a tension of ~14 pN. Around this force, the translocation rate of T7 helicase does not show a strong dependence on force on the ssDNA (Johnson et al., 2007).

3.4 Polymerase Strand Displacement Assay

Replicative DNAPs are responsible for faithfully synthesizing genomic DNA, in both prokaryotes and eukaryotes, by adding nucleotides to the 3′ terminus of the primer strand. To increase the fidelity of DNA replication, replicative DNAPs typically have a 3′–5′ exonuclease to allow for proofreading by excision of erroneous incorporated nucleotides. DNAP's activity can be measured with a strand displacement assay in which DNAP carries leading-strand synthesis while displacing the lagging strand at a DNA fork. As the DNA fork is typically an obstacle for DNAP, a force assisting strand separation will facilitate the advancement of DNAPs (Fig. 5A). Here, using T7 DNAP as an example, we detail the experimental procedures of the strand displacement assay on the aforementioned DNA template (Sun et al., 2015). Wild-type (wt) DNAP (NEB) contains gp5 and trx and can be used directly. Exo^- DNAP is assembled by adding 10 μ*M* of gp5 to 50 μ*M E. coli* trx and incubating at room temperature for 5 min. Before data

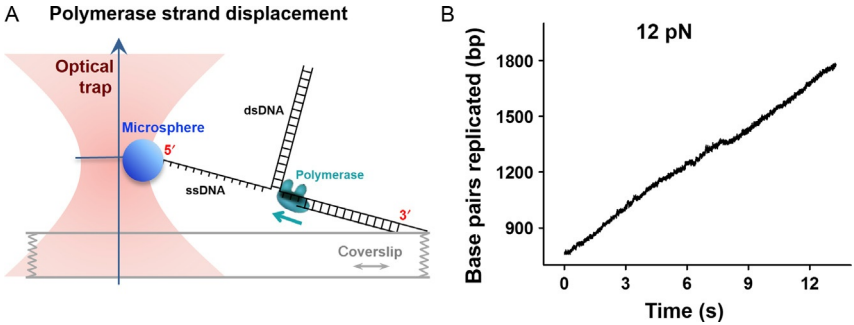

Fig. 5 Polymerase strand displacement assay. (A) Experimental configuration for the polymerase strand displacement assay. This cartoon illustrates the experimental configuration for the observation of DNA synthesis by a single T7 DNAP as it displaces the other strand. (B) A representative trace showing the number of replicated base pairs vs time in the presence of 1 m*M* dNTPs under 12 pN.

acquisition, the appropriate DNAP is diluted in its reaction buffer (50 m*M* Tris–HCl pH 7.5, 40 m*M* NaCl, 10% glycerol, 1.5 m*M* EDTA, 2 m*M* DTT, 8 m*M* $MgCl_2$, and 1 m*M* dNTP each) to 30 n*M*, before flowing it into the chamber. The experimental procedure is similar to the helicase-unwinding assay:

(1) Mechanically unzipping to generate ssDNA. At a constant velocity, several hundred base pairs of dsDNA are mechanically unzipped to produce a region of ssDNA as a template for the polymerase.

(2) Polymerase loading. DNA length is maintained under a "hold" mode until a force drop is observed, indicating polymerase unwinding of the DNA fork.

(3) Polymerase unwinding/synthesizing under constant force. The setup then switches to a "force clamp" mode to maintain a constant force, while a polymerase unwinds and synthesizes the downstream dsDNA.

It is worth noting here that wt T7 DNAP has force-dependent synthesis and exonuclease activities. Under a force less than 8 pN, exonuclease activity dominates under the influence of the reannealing fork, and this leads to a decrease in DNA extension corresponding to a decrease in the number of base pairs replicated (see later). At higher forces, this effect is significantly alleviated, and thus wt T7 DNAP can perform strand displacement synthesis (Fig. 5B).

The experimental configuration and DNA template design detailed ealier provide several advantages for detecting the motion of helicase and polymerase. First, the motor protein of interest does not need to be tagged

or anchored, nor under direct mechanical stress, minimizing potential perturbation to the protein. Second, for proteins that can only associate with ssDNA, experiments can only be initiated after a ssDNA loading region is mechanically generated. Thus, the start of an experiment on each DNA molecule can be independently controlled. Third, for both helicase unwinding and polymerase synthesis assays, each base pairs of dsDNA unwound results in the release of 2 nt ssDNA (for helicase) or 1 nt ssDNA and 1 bp dsDNA (for polymerase), amplifying the detection signal.

Using this method, we have directly measured the dynamic activities of individual proteins in the replisome (Johnson et al., 2007; Sun et al., 2011, 2015). Next, we expand this approach to investigate multicomponent, dynamic machineries of the T7 replisome, namely, more than one protein is investigated at any one time during replication.

4. SINGLE-MOLECULE STUDIES OF THE RESPONSE OF A REPLISOME TO DNA DAMAGE

DNA replication often relies on DNA damage tolerance pathways to overcome DNA damage which, if not repaired, may cause a replication fork to stall or collapse, leading to genomic instability and cell death. In order to complete the cell cycle and maintain cell survival, it is often more advantageous to circumvent blocked replication forks and postpone the damage repair (Yeeles, Poli, Marians, & Pasero, 2013). Thus, a detailed understanding of the response of a replisome to DNA damage, as well as possible lesion tolerance pathways, is of great interest to multiple fields, including genome stability, cell survival, and human disease (Zeman & Cimprich, 2014).

Previous studies showed that the translocation of T7 helicase on ssDNA was blocked by bulky DNA adducts (Brown & Romano, 1989). Therefore, damage to DNA could interfere with the helicase in its translocation or unwinding, leading to the stalled or collapsed replication fork. T7 DNAP belongs to the high-fidelity Pol A family of polymerases and is unable to bypass UV-induced lesions on its own. However, the exonuclease-deficient (exo^-) T7 DNAP mutant is able to bypass them, suggesting its proofreading activity is important in its ability to bypass a lesion (McCulloch & Kunkel, 2006; Smith, Baeten, & Taylor, 1998). These processes are highly dynamic, which is often averaged out in the classical biochemical experiments. Thus, we have developed single-molecule methods to investigate these questions (Sun et al., 2015).

4.1 DNA Template Design and Construction

To monitor the real-time dynamic process of DNA replication and investigate the response of each replicative protein after encountering a lesion, we designed a Y-shaped DNA template containing a single *cis–syn* cyclobutane pyrimidine dimer (CPD) lesion in either the leading-strand or lagging-strand of a forked DNA template (Inman et al., 2014; Sun et al., 2015). Although we use CPD as an example, the methods described here could be easily applied to other types of lesions. This DNA template consists of three distinct dsDNA segments: two arms and a trunk (Fig. 6). The two arms can be amplified from plasmids with end-labeled tags, followed by restriction enzyme cuts to create overhangs for subsequent ligation. The trunk is, itself, a ligation product of a three-piece segment: upstream segment, lesion segment, and downstream segment. The upstream and downstream segments are made via PCR amplification of plasmids, and ligation overhangs are generated by restriction enzyme digest. The two arms and the trunk are linked via three adapter oligonucleotides, and upon ligation, form Y-shaped DNA template. The resulting template provides an artificial replication fork containing a ssDNA loading region for the replisome to load and replicate. Here, we provide a detailed procedure to construct this lesion-containing DNA template (Fig. 6):

Arms preparation (Fig. 6A)

(1) Arm 1 (1.1 kbp) is amplified from plasmid pLB574 using a digoxigenin-labeled primer. Arm 2 (2 kbp) is amplified from plasmid pBR322 (NEB) using a biotin-labeled primer.

(2) Arm 1 and Arm 2 PCR products are digested with BstXI (NEB) and BstEII (NEB), respectively, to create overhangs for adapter ligation.

(3) Arm 1 is annealed to a short DNA at 1:10 molar ratio at 16°C for at least 4 h. The short DNA is an annealing product of two adapters (adapters 1 and 2) with an overhang complementary to that of Arm 1. Ligation products are purified using agarose gel purification kit (Zymo Research).

(4) Arm 2 is annealed to adapter 3 at 1:10 molar ratio, and gel purified to eliminate excess adapters.

(5) Adapter 2 from Arm 1 (step 3) and adapter 3 from Arm 2 (step 4) are partially complementary to each other and are annealed to create a replication fork with a short 30-bp trunk with 3-bp overhang for subsequent ligation to the trunk segment.

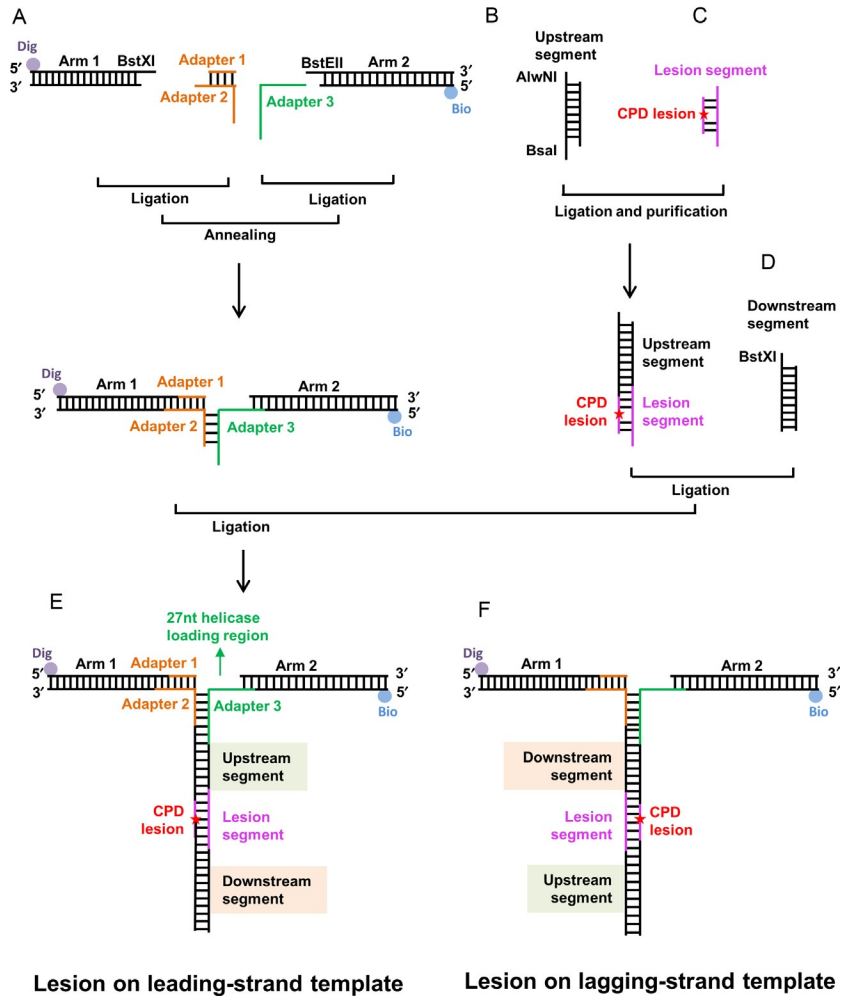

Fig. 6 Lesion-containing template construction. A DNA template for studies of the response of a replisome to a DNA lesion is illustrated. Two arms are linked via three adapters (A). The trunk consists of an upstream segment (B), a lesion-containing segment (C), and a downstream segment (D). The final DNA template with a lesion located on the leading strand (E) or the lagging strand (F) is a ligation product of two arms and a trunk. See text for a detailed description of the procedures.

Trunk preparation

(6) For the trunk, a 1.1-kbp upstream (Fig. 6B) and 1.1-kbp downstream segment (Fig. 6D) are amplified via PCR from a pRL574 plasmid variant.

(7) The upstream and downstream PCR products are then cut by BsaI and BstXI (NEB), respectively, to create overhangs for ligation with the lesion segment.

(8) The lesion segment (Fig. 6C) is made by annealing a CPD lesion-containing oligonucleotide with its complementary oligonucleotide. Of note, the *cis–syn* cyclobutane thymine dimer phosphoramidite is purchased from Glen Research (Sterling, VA) and was used for synthesis of the CPD oligonucleotide with PAGE purification by Oligos Etc (Wilsonville, OR). The upstream segment, the lesion segment, and the downstream segment are ligated and purified using gel purification.

Arms and trunk ligation

(9) To create a DNA template with a CPD lesion located on the leading-strand template, the upstream DNA segment is also digested with AlwNI (NEB) before ligation with the lesion segment. This creates an overhang for ligation with arms and results in a CPD lesion located at 1145–1146 bp from the initial fork (Fig. 6E). To create the DNA template with a CPD lesion located on the lagging-strand template, the trunk sequence was flipped, and the downstream DNA segment, instead of the upstream DNA segment, is digested with AlwNI (NEB) to create an overhang for ligation with the arms, resulting in a CPD lesion located at 1223–1224 bp from the initial fork (Fig. 6F). Arms are ligated with the trunk at 1:4 molar ratio under 16°C for 3 h on the day of an experiment.

4.2 Response of Individual Proteins to DNA Damage: Helicase-Unwinding Assay and Polymerase Strand Displacement Assay.

To investigate the response of the bacteriophage T7 replisome to a DNA lesion, the effect of the lesion on individual proteins need to be first examined (Fig. 7) (Sun et al., 2015). Helicase unwinding and polymerase strand displacement experiments are conducted as previously described in Sections 3.2 and 3.4. In brief, several hundred base pairs of dsDNA before the lesion are mechanically unzipped (with an average unzipping force of ~15 pN), at a constant velocity of 1400 nm/s, to produce a ssDNA loading region for helicase or a template for polymerase. Then, DNA length is maintained until a force drop is observed (below a predetermined threshold), indicating helicase or polymerase unwinding of the DNA fork. Subsequently, a constant force is maintained, while helicase or polymerase

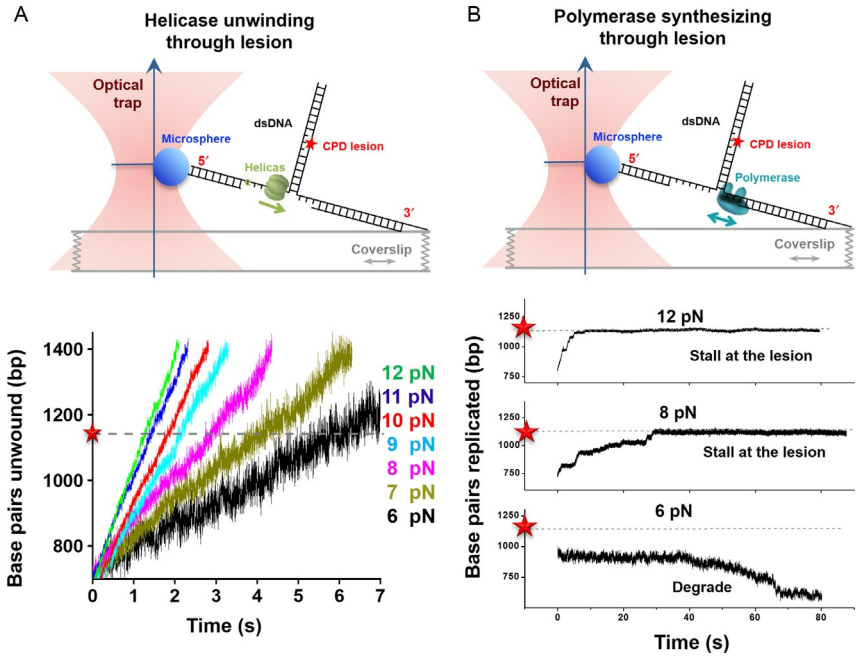

Fig. 7 Helicase unwinding and polymerase synthesizing through a *cis–syn* CPD lesion. (A) Helicase unwinding through a CPD lesion. This cartoon illustrates the experimental configuration for the observation of T7 helicase unwinding through a CPD lesion. A CPD lesion (*red star*) is located in the leading-strand DNA. Representative traces show the number of unwound base pairs vs time in the presence of 2 m*M* dTTP. (B) Polymerase synthesizing through a CDP lesion. The cartoon illustrates the experimental configuration for the observation of T7 DNAP synthesizing through a CPD lesion. Representative traces show the number of replicated base pairs vs time in the presence of 1 m*M* dNTPs under 12, 8, and 6 pN. Note that at 6 pN, DNAP excised DNA from the 3′ end. The *dotted lines* indicate the lesion position. *Adapted from Sun, B., Pandey, M., Inman, J. T., Yang, Y., Kashlev, M., Patel, S. S., et al. (2015). T7 replisome directly overcomes DNA damage.* Nature Communications*, 6, 10260, with permission from the publisher.*

unwinds the dsDNA. To be consistent, both experiments are conducted in a replication buffer which consists of 50 m*M* Tris–HCl (pH 7.5), 40 m*M* NaCl, 10% glycerol, 1.5 m*M* EDTA, 2 m*M* DTT and 1 m*M* dNTPs (each), and 8 m*M* $MgCl_2$. For the helicase-unwinding assay, 0.4 n*M* hexamer helicase is typically used to ensure single helicase conditions. For the strand displacement assay, 30 n*M* of the appropriate DNAP in 50 μL replication buffer is flowed into the chamber before data acquisition.

4.3 Response of a Replisome to DNA Damage: Leading-Strand Replication Assay

The leading-strand replication assay is performed under a "force clamp" (Fig. 8A) (Sun et al., 2015). To avoid strand displacement synthesis by DNAP alone, the experiments are conducted under a low force of 6 pN where T7 DNAP exonuclease activity alone would lead to a decrease in DNA length. Therefore, the DNA length increase would only be due to either helicase unwinding or helicase/DNAP replication under this condition. These two scenarios are differentiated by the rate of the DNA length increase which is utilized to determine the fates of the proteins after the lesion (see Section 5.4 for details). The helicase and polymerase are prepared as follows: first, 30 n*M* of the appropriate helicase hexamer is incubated for 10 min, on ice, in the replication buffer, then 30 n*M* of the appropriate DNAP is added, and the solution is incubated for 10 min at room temperature. The resulting 50 μL solution is flowed into a chamber just before data acquisition. The DNA template design contains a 27-nt initial ssDNA region (Fig. 6E) that accommodates only one helicase with one DNAP loaded at the fork, as each T7 helicase has been shown to bind and protect 25–30 bases of ssDNA (Egelman, Yu, Wild, Hingorani, & Patel, 1995; Hingorani & Patel, 1993; Patel & Hingorani, 1993). The low concentrations of helicase and DNAP, added at a stoichiometric ratio, ensure that the experiments are likely to occur under a single copy conditions.

5. DATA ANALYSIS

After the acquired data signals are converted into force and DNA extension, the data need to be further processed as described below.

5.1 DNA Elastic Parameter Determination

Elasticity parameters, of both dsDNA and ssDNA, are necessary for data conversion and are obtained from the DNA force–extension measurements. They are strongly dependent on the buffer conditions used in the experiments. The force–extension relation of dsDNA was obtained by stretching dsDNA in the same replication buffer mentioned earlier and fit by using a modified Marko–Siggia worm-like-chain model (Wang, Yin, Landick, Gelles, & Block, 1997). The fit yielded the following fitting parameter values (Sun et al., 2015): the contour length per base is 0.338 nm, the persistence length of DNA is 44.5 nm, and the stretch modulus is 1200 pN.

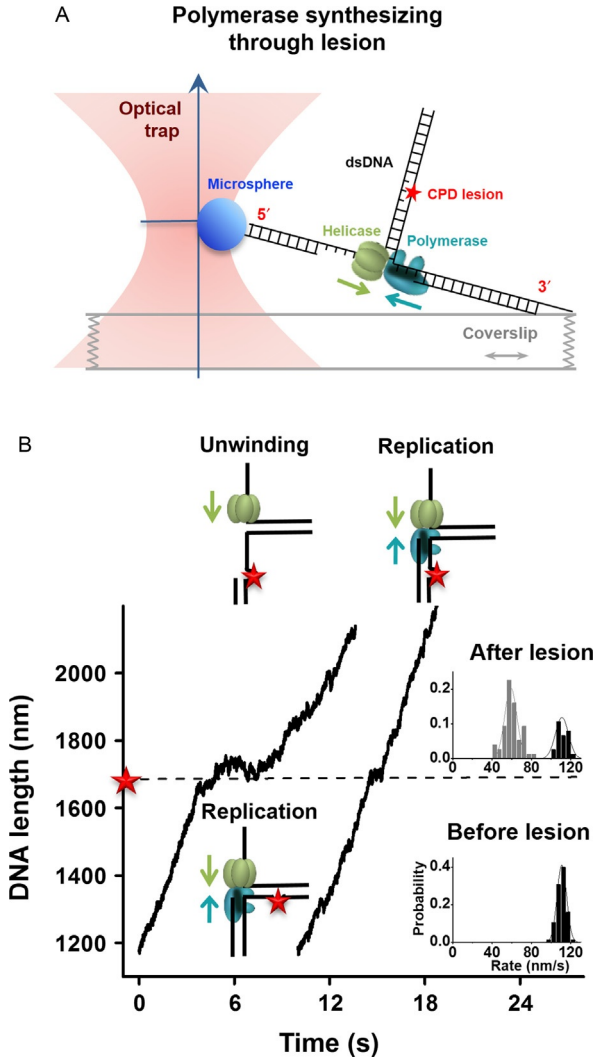

Fig. 8 Leading-strand synthesis on a DNA template containing a CPD lesion in the presence of helicase. (A) Experimental configuration. This cartoon illustrates the experimental configuration for the observation of leading-strand synthesis through a CPD lesion (*red star*). (B) Representative traces showing DNA length vs time for a wt DNAP with helicase in the presence of 0.5 m*M* dNTPs and 6 pN. The *dotted lines* indicate the position of a single CPD lesion. For clarity, traces have been shifted along the time axis. Cartoons illustrate different protein compositions at the fork before and after the lesion for each trace. Insets display the distributions of DNA length increase rates before and after the lesion. *Adapted from Sun, B., Pandey, M., Inman, J. T., Yang, Y., Kashlev, M., Patel, S. S., et al. (2015). T7 replisome directly overcomes DNA damage.* Nature Communications*, 6, 10260, with permission from the publisher.*

The force–extension relation of ssDNA may be described by an extensible freely jointed chain (FJC) model (Smith, Cui, & Bustamante, 1996). For forces higher than 12 pN, this relation may be obtained using an unzipping template with a hairpin at its distal end (Johnson et al., 2007). Upon mechanically unzipping all the way to the hairpin to generate ssDNA, the ssDNA may then be stretched to obtain the force–extension curve of the ssDNA. The resulting force extension is well fit by the FJC model, yielding a contour length per base of 0.52 nm, a Kuhn's length of 1.91 nm and a stretch modulus of 393 pN. For forces lower than 12 pN, the force extension is directly determined using a helicase-based method (Johnson et al., 2007). In brief, the helicase loads onto the ssDNA and starts to unwind dsDNA under a constant force. This is followed by stretching the two ends of the DNA, at 1400 nm/s to 13 pN, which is sufficient to remove any secondary structures in the ssDNA. The force increase is rapid so that the helicase is not expected to move forward by more than a few base pair during this time. Thus, the force–extension measurements could then be used to determine the number of ssDNA base pairs at the force prior to stretching. Setting different constant low forces for the initial dsDNA unwinding by the helicase allows the determination of the force–extension curve of ssDNA over the entire range of relevant forces. The resulting curve may be fit with a polynomial (Johnson et al., 2007).

5.2 DNA Extension Conversion to Number of Base Pairs

For the helicase-unwinding studies, one base pair unwound generates two nucleotides of ssDNA. Accordingly, real-time DNA extension under a given force is converted into the number of base pairs unwound (Johnson et al., 2007). To improve positional accuracy and precision, the data during the initial mechanically unzipping are used to align to a theoretical unzipping curve (Dechassa et al., 2011; Deufel & Wang, 2006; Hall et al., 2009; Inman et al., 2014; Jiang et al., 2005; Jin et al., 2010; Johnson et al., 2007; Li & Wang, 2012; Li et al., 2015; Shundrovsky et al., 2006). For the DNAP strand displacement synthesis studies, one separated base pair is converted into one base pair of dsDNA, via DNA synthesis, and one nucleotide of ssDNA. Accordingly, DNA extension under a given force is converted into the number of nucleotides synthesized, or excised, by DNAP (Sun et al., 2015). In particular, under 6 pN of force, a 1 nm increase in length corresponded to 1.95 bp unwound by helicase and 1.74 bp replicated by the leading-strand synthesis.

To determine the expected lesion position in the extension signal on a lesion-containing template in the leading-strand replication assay, the DNA template before the lesion is assumed to be replicated, and the lesion position in base pairs which is known from the DNA template design is converted into extension (in nanometer).

5.3 Helicase Slippage Determination and Processivity Measurements

In the helicase-unwinding assay, when ATP is used, a remarkable sawtooth pattern in the unwinding trace is observed as processive unwinding is interrupted by slippage events. The slippage events are due to helicase losing its grip on the ssDNA, and sliding backwards under the influence of the reannealing DNA fork (Sun et al., 2011). We set a threshold of 2000 bp/s, in the reverse velocity, for identifying slippage. Distances that a helicase travels between slips are compiled to determine processivity (Fig. 9A), and the distances follow an exponential distribution, indicating a stochastic process in slippage.

5.4 Unwinding Rate and Replication Rate Measurements and Comparison

For the sequence-dependent helicase-unwinding studies, to improve positional accuracy and precision to a few base pairs, the initial mechanical unzipping section of each trace was aligned with the theoretical prediction (Johnson et al., 2007; Sun et al., 2011). After alignment, an instantaneous unwinding rate at each sequence position is determined using a Gaussian weighted filter of 0.05 s and then resampling at 1-bp intervals along the sequence position. The final rate vs position curve is found by averaging each position over all of the traces.

For the leading-strand replication studies, one first has to determine whether the extension change is due to the helicase alone or DNAP synthesis coupled with helicase unwinding. The differentiation is achieved by directly measuring and comparing the length increase rates in nanometer per second on an unmodified DNA template (Sun et al., 2015). The average rates are found from linear fits to each trace, followed by averaging over all of the traces. Taking the experiments using 0.5 m*M* dNTP (each) and 6 pN as an example, the unwinding by helicase alone results in a DNA length increase at rate of 63 ± 22 nm/s, and when DNAP is present together with helicase, the rate increases to 111 ± 13 nm/s (Sun et al., 2015). Subsequently, depending on whether the DNA template is replicated, the rates

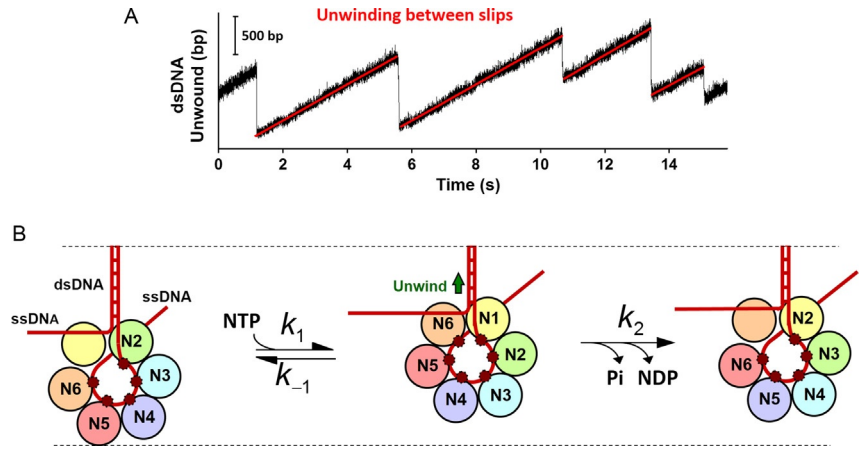

Fig. 9 Helicase slippage and a proposed coordinated model. (A) An example of unwinding with ATP to illustrate the method of determining distance between slips. (B) Hexameric helicase subunit coordination. Each subunit is uniquely labeled with a *different color* and has a potential ssDNA-binding site (*small dots*). Nucleotide binding and subsequent hydrolysis occur sequentially around the ring. If a subunit is nucleotide ligated (the state of hydrolysis indicated by Ni), it has a nonzero probability of being bound to ssDNA. During unwinding, the leading subunit can bind to a nucleotide (N) and thus acquire affinity for the downstream ssDNA. This stimulates the last nucleotide-bound subunit to release its nucleotide and ssDNA. Then, the cycle proceeds again around the ring. Slippage occurs when all subunits simultaneously release ssDNA. *Adapted from Sun, B., Johnson, D. S., Patel, G., Smith, B. Y., Pandey, M., Patel, S. S., et al. (2011). ATP-induced helicase slippage reveals highly coordinated subunits.* Nature, 478, *132–135, with permission from the publisher.*

in nanometer per second can be converted into base pairs per second using the elastic parameters of both ssDNA and dsDNA.

5.5 Fate of a Replisome Encountering DNA Damage

As mentioned earlier, to examine the fate of a replisome encountering DNA damage, one has to determine whether the postlesion movement of the fork is due to the helicase alone or DNAP synthesis coupled with helicase unwinding. The length increase rate after the lesion is measured by a linear fit to the unwinding trace and then compared with the rates obtained from the unmodified template (Sun et al., 2015). DNAP may terminate synthesizing after the lesion but still associate with the helicase and alter its unwinding rate. To mimic this condition, the control experiments to measure helicase-unwinding rates are conducted in the presence of

DNAP by using a modified template with a 3′ inverted dT incorporated at the adapter 1 (IDT) from which DNAP could not synthesize (Sun et al., 2015).

6. UNIQUE FEATURES OF THE BACTERIOPHAGE T7 REPLISOME REVEALED BY SINGLE-MOLECULE OPTICAL-TRAPPING TECHNIQUES

Here, we summarize major results obtained from the studies of the bacteriophage T7 replisome using single-molecule optical-trapping techniques. For more specific details regarding these experiments, or data analysis, we refer the reader to the original publications (Sun et al., 2011, 2015).

6.1 Helicase Slippage and Subunit Coordination

T7 helicase is a model hexameric helicase that uses dTTP to unwind dsDNA. Earlier bulk studies of T7 helicase found that although T7 helicase is capable of ATP hydrolysis, it did not unwind DNA efficiently in the presence of ATP (Hingorani & Patel, 1996; Matson & Richardson, 1983). Our single-molecule results revealed that ATP supported not only dsDNA unwinding but also a significantly faster unwinding rate than that with dTTP (Sun et al., 2011). However, in the presence of ATP, helicase unwinding is frequently interrupted by slippage, where helicase loses the grip of ssDNA, moves in a reverse direction along the ssDNA, but then regains the grip of ssDNA before moving forward again. These results have resolved the mystery of the apparent lack of significant unwinding activity seen in bulk studies, as the frequent slippage prevents helicase from moving over a substantial distance to be detected in a strand separation assay. Thus far, T7 helicase is the only motor protein that has reported nucleotide-specific slippage behavior. Slippage has been observed with other helicases, however, it appears to result from different causes (Klaue et al., 2013; Lee et al., 2014; Manosas, Spiering, Ding, Croquette, & Benkovic, 2012; Myong, Bruno, Pyle, & Ha, 2007; Myong, Rasnik, Joo, Lohman, & Ha, 2005; Qi, Pugh, Spies, & Chemla, 2013; Sun et al., 2008).

More importantly, these slippage events provided us with a unique opportunity to investigate how different subunits of the helicase coordinate their mechanical and chemical activities (Sun et al., 2011). By examining the helicase processivity in a mixture of ATP and dTTP in conjunction with theoretical modeling, we found that all, or nearly all, six of subunits of the helicase must coordinate their mechanochemical activities. Based on

structural studies of hexameric ring-shaped helicases E1 and Rho (Enemark & Joshua-Tor, 2006; Thomsen & Berger, 2009), we proposed a mechanistic model for T7 helicase. In this model, coordination could occur sequentially around the hexameric ring with the leading subunit poised for NTP binding and each successive subunit having a bound nucleotide in states of progression along the chemical reaction pathway. Once the leading subunit binds to an NTP and reels in the DNA, the remaining subunits progress to their next reaction states. Product release by the last participating subunit results in release of DNA from that subunit, and thus completes a single cycle (Fig. 9B). It is speculated that slippage may provide an evolutionary advantage for replication and allow helicase synchronization with a nonsynthesizing or slow-moving DNAP.

6.2 Inherent Tolerance of the T7 Replisome to DNA Damage

Leading-strand DNA lesions are often major obstacles for replication progression, as the high-fidelity replicative polymerase is incapable of directly proceeding through them. As examples, for both T4 and *E. coli* replisomes, leading- and lagging-strand DNA replication becomes uncoupled after encountering a leading-strand DNA lesion (Higuchi et al., 2003; McInerney & O'Donnell, 2007; Nelson & Benkovic, 2010). A replisome often adopts an indirect pathway to tolerate DNA damage, which requires the replisome to avoid lesions and/or reinitiate replication after bypass (Yeeles & Marians, 2011; Yeeles et al., 2013). Using the techniques mentioned earlier, we examined how T7 helicase and polymerase deal with a UV-induced CPD lesion in the leading-strand template (Sun et al., 2015). We demonstrated that, in the presence of T7 helicase, a substantial fraction of T7 DNAP is able to replicate through the lesion directly. The helicase and the polymerase replicate up to the lesion and stay together to synthesize through the lesion through specific helicase–DNAP interactions. Upon lesion bypass, DNAP and the helicase concurrently resume their independent activities (Fig. 8C). These results suggest that the T7 replisome is fundamentally permissive of DNA lesions. This is, to our knowledge, the first observation of CPD tolerance by a helicase-coupled replicative polymerase synthesizing through a lesion, rather than circumventing it. Based on these results, we proposed a new lesion bypass pathway, in which a replicative DNAP directly synthesizes through a leading-strand lesion with the assistance of a helicase. In contrast to other pathways, the new pathway functions in the absence of additional accessory proteins, with the exception of

helicase, and replication fork adjustment and reinitiation of the replisome are not required. Therefore, it is more efficient in terms of replisome recovery.

7. CONCLUSIONS

Single-molecule optical-trapping techniques have expanded to impact a wide field of biological sciences. The experimental methods detailed here offer the ability to resolving helicase or polymerase motion at high spatial and temporal resolution, generating a more comprehensive understanding of these motor proteins and their corresponding functions in the replisome during replication. The detailed experimental design mentioned here provides an opportunity to monitor the dynamics of the multicomponent machinery of a replisome and is capable of elucidating the cooperation and coordination of two or more proteins simultaneously. We anticipate that this method will continue to play an important role in the study of proteins and molecular machines and will be further enhanced in combination with other single-molecule techniques.

ACKNOWLEDGMENTS

We thank Dr. Shanna M. Moore from the Wang Laboratory at Cornell University for critical comments on the manuscript. We wish to acknowledge support from Shanghai Pujiang Program (16PJ1406900 to B.S.), National Key Research and Development Program of China (2016YFA0500900 to B.S.) and National Science Foundation Grant (MCB-1517764 to M.D.W.).

REFERENCES

Ahnert, P., & Patel, S. S. (1997). Asymmetric interactions of hexameric bacteriophage T7 DNA helicase with the 5′- and 3′-tails of the forked DNA substrate. *The Journal of Biological Chemistry*, *272*, 32267–32273.

Benkovic, S. J., Valentine, A. M., & Salinas, F. (2001). Replisome-mediated DNA replication. *Annual Review of Biochemistry*, *70*, 181–208.

Brower-Toland, B., & Wang, M. D. (2004). Use of optical trapping techniques to study single-nucleosome dynamics. *Methods in Enzymology*, *376*, 62–72.

Brown, W. C., & Romano, L. J. (1989). Benzo[a]pyrene-DNA adducts inhibit translocation by the gene 4 protein of bacteriophage T7. *The Journal of Biological Chemistry*, *264*, 6748–6754.

Dechassa, M. L., Wyns, K., Li, M., Hall, M. A., Wang, M. D., & Luger, K. (2011). Structure and Scm3-mediated assembly of budding yeast centromeric nucleosomes. *Nature Communications*, *2*, 313.

Deufel, C., & Wang, M. D. (2006). Detection of forces and displacements along the axial direction in an optical trap. *Biophysical Journal*, *90*, 657–667.

Donmez, I., & Patel, S. S. (2006). Mechanisms of a ring shaped helicase. *Nucleic Acids Research*, *34*, 4216–4224.

Donmez, I., & Patel, S. S. (2008). Coupling of DNA unwinding to nucleotide hydrolysis in a ring-shaped helicase. *The EMBO Journal*, *27*, 1718–1726.
Egelman, E. H., Yu, X., Wild, R., Hingorani, M. M., & Patel, S. S. (1995). Bacteriophage T7 helicase/primase proteins form rings around single-stranded DNA that suggest a general structure for hexameric helicases. *Proceedings of the National Academy of Sciences of the United States of America*, *92*, 3869–3873.
Enemark, E. J., & Joshua-Tor, L. (2006). Mechanism of DNA translocation in a replicative hexameric helicase. *Nature*, *442*, 270–275.
Hall, M. A., Shundrovsky, A., Bai, L., Fulbright, R. M., Lis, J. T., & Wang, M. D. (2009). High-resolution dynamic mapping of histone-DNA interactions in a nucleosome. *Nature Structural & Molecular Biology*, *16*, 124–129.
Hamdan, S. M., & Richardson, C. C. (2009). Motors, switches, and contacts in the replisome. *Annual Review of Biochemistry*, *78*, 205–243.
Higuchi, K., Katayama, T., Iwai, S., Hidaka, M., Horiuchi, T., & Maki, H. (2003). Fate of DNA replication fork encountering a single DNA lesion during oriC plasmid DNA replication in vitro. *Genes to Cells*, *8*, 437–449.
Hingorani, M. M., & Patel, S. S. (1993). Interactions of bacteriophage T7 DNA primase/helicase protein with single-stranded and double-stranded DNAs. *Biochemistry*, *32*, 12478–12487.
Hingorani, M. M., & Patel, S. S. (1996). Cooperative interactions of nucleotide ligands are linked to oligomerization and DNA binding in bacteriophage T7 gene 4 helicases. *Biochemistry*, *35*, 2218–2228.
Inman, J. T., Smith, B. Y., Hall, M. A., Forties, R. A., Jin, J., Sethna, J. P., et al. (2014). DNA Y structure: A versatile, multidimensional single molecule assay. *Nano Letters*, *14*, 6475–6480.
Jiang, J., Bai, L., Surtees, J. A., Gemici, Z., Wang, M. D., & Alani, E. (2005). Detection of high-affinity and sliding clamp modes for MSH2–MSH6 by single-molecule unzipping force analysis. *Molecular Cell*, *20*, 771–781.
Jin, J., Bai, L., Johnson, D. S., Fulbright, R. M., Kireeva, M. L., Kashlev, M., et al. (2010). Synergistic action of RNA polymerases in overcoming the nucleosomal barrier. *Nature Structural & Molecular Biology*, *17*, 745–752.
Johnson, D. S., Bai, L., Smith, B. Y., Patel, S. S., & Wang, M. D. (2007). Single-molecule studies reveal dynamics of DNA unwinding by the ring-shaped T7 helicase. *Cell*, *129*, 1299–1309.
Kim, Y. T., & Richardson, C. C. (1993). Bacteriophage T7-gene 2.5-protein—An essential protein for DNA-replication. *Proceedings of the National Academy of Sciences of the United States of America*, *90*, 10173–10177.
Klaue, D., Kobbe, D., Kemmerich, F. E., Kozikowska, A., Puchta, H., & Seidel, R. (2013). Fork sensing and strand switching control antagonistic activities of RecQ helicases. *Nature Communications*, *4*, 2024.
Koch, S. J., Shundrovsky, A., Jantzen, B. C., & Wang, M. D. (2002). Probing protein-DNA interactions by unzipping a single DNA double helix. *Biophysical Journal*, *83*, 1098–1105.
Koch, S. J., & Wang, M. D. (2003). Dynamic force spectroscopy of protein-DNA interactions by unzipping DNA. *Physical Review Letters*, *91*, 028103.
Lee, S. J., & Richardson, C. C. (2010). Molecular basis for recognition of nucleoside triphosphate by gene 4 helicase of bacteriophage T7. *The Journal of Biological Chemistry*, *285*, 31462–31471.
Lee, S. J., Syed, S., Enemark, E. J., Schuck, S., Stenlund, A., Ha, T., et al. (2014). Dynamic look at DNA unwinding by a replicative helicase. *Proceedings of the National Academy of Sciences of the United States of America*, *111*, E827–E835.
Li, M., Hada, A., Sen, P., Olufemi, L., Hall, M. A., Smith, B. Y., et al. (2015). Dynamic regulation of transcription factors by nucleosome remodeling. *eLife*, *4*, e06249.

Li, M., & Wang, M. D. (2012). Unzipping single DNA molecules to study nucleosome structure and dynamics. *Methods in Enzymology*, *513*, 29–58.
Manosas, M., Spiering, M. M., Ding, F., Croquette, V., & Benkovic, S. J. (2012). Collaborative coupling between polymerase and helicase for leading-strand synthesis. *Nucleic Acids Research*, *40*, 6187–6198.
Matson, S. W., & Richardson, C. C. (1983). DNA-dependent nucleoside 5′-triphosphatase activity of the gene 4 protein of bacteriophage T7. *The Journal of Biological Chemistry*, *258*, 14009–14016.
Matson, S. W., Tabor, S., & Richardson, C. C. (1983). The gene 4 protein of bacteriophage T7. Characterization of helicase activity. *The Journal of Biological Chemistry*, *258*, 14017–14024.
McCulloch, S. D., & Kunkel, T. A. (2006). Multiple solutions to inefficient lesion bypass by T7 DNA polymerase. *DNA Repair*, *5*, 1373–1383.
McInerney, P., & O'Donnell, M. (2007). Replisome fate upon encountering a leading strand block and clearance from DNA by recombination proteins. *The Journal of Biological Chemistry*, *282*, 25903–25916.
Moffitt, J. R., Chemla, Y. R., Smith, S. B., & Bustamante, C. (2008). Recent advances in optical tweezers. *Annual Review of Biochemistry*, *77*, 205–228.
Myong, S., Bruno, M. M., Pyle, A. M., & Ha, T. (2007). Spring-loaded mechanism of DNA unwinding by hepatitis C virus NS3 helicase. *Science*, *317*, 513–516.
Myong, S., Rasnik, I., Joo, C., Lohman, T. M., & Ha, T. (2005). Repetitive shuttling of a motor protein on DNA. *Nature*, *437*, 1321–1325.
Nelson, S. W., & Benkovic, S. J. (2010). Response of the bacteriophage T4 replisome to noncoding lesions and regression of a stalled replication fork. *Journal of Molecular Biology*, *401*, 743–756.
Patel, S. S., & Hingorani, M. M. (1993). Oligomeric structure of bacteriophage T7 DNA primase/helicase proteins. *The Journal of Biological Chemistry*, *268*, 10668–10675.
Patel, G., Johnson, D. S., Sun, B., Pandey, M., Yu, X., Egelman, E. H., et al. (2011). A257T linker region mutant of T7 helicase-primase protein is defective in DNA loading and rescued by T7 DNA polymerase. *The Journal of Biological Chemistry*, *286*, 20490–20499.
Qi, Z., Pugh, R. A., Spies, M., & Chemla, Y. R. (2013). Sequence-dependent base pair stepping dynamics in XPD helicase unwinding. *eLife*, *2*, e00334.
Shundrovsky, A., Smith, C. L., Lis, J. T., Peterson, C. L., & Wang, M. D. (2006). Probing SWI/SNF remodeling of the nucleosome by unzipping single DNA molecules. *Nature Structural & Molecular Biology*, *13*, 549–554.
Singleton, M. R., Dillingham, M. S., & Wigley, D. B. (2007). Structure and mechanism of helicases and nucleic acid translocases. *Annual Review of Biochemistry*, *76*, 23–50.
Smith, C. A., Baeten, J., & Taylor, J. S. (1998). The ability of a variety of polymerases to synthesize past site-specific cis-syn, trans-syn-II, (6–4), and Dewar photoproducts of thymidylyl-(3′–>5′)-thymidine. *Journal of Biological Chemistry*, *273*, 21933–21940.
Smith, S. B., Cui, Y., & Bustamante, C. (1996). Overstretching B-DNA: The elastic response of individual double-stranded and single-stranded DNA molecules. *Science*, *271*, 795–799.
Sun, B., Johnson, D. S., Patel, G., Smith, B. Y., Pandey, M., Patel, S. S., et al. (2011). ATP-induced helicase slippage reveals highly coordinated subunits. *Nature*, *478*, 132–135.
Sun, B., Pandey, M., Inman, J. T., Yang, Y., Kashlev, M., Patel, S. S., et al. (2015). T7 replisome directly overcomes DNA damage. *Nature Communications*, *6*, 10260.
Sun, B., & Wang, M. D. (2016). Single-molecule perspectives on helicase mechanisms and functions. *Critical Reviews in Biochemistry and Molecular Biology*, *51*, 15–25.
Sun, B., Wei, K. J., Zhang, B., Zhang, X. H., Dou, S. X., Li, M., et al. (2008). Impediment of *E. coli* UvrD by DNA-destabilizing force reveals a strained-inchworm mechanism of DNA unwinding. *The EMBO Journal*, *27*, 3279–3287.

Tabor, S., Huber, H. E., & Richardson, C. C. (1987). Escherichia coli thioredoxin confers processivity on the DNA polymerase activity of the gene 5 protein of bacteriophage T7. *The Journal of Biological Chemistry*, *262*, 16212–16223.

Thomsen, N. D., & Berger, J. M. (2009). Running in reverse: The structural basis for translocation polarity in hexameric helicases. *Cell*, *139*, 523–534.

Wang, M. D., Yin, H., Landick, R., Gelles, J., & Block, S. M. (1997). Stretching DNA with optical tweezers. *Biophysical Journal*, *72*, 1335–1346.

Yeeles, J. T. P., & Marians, K. J. (2011). The Escherichia coli replisome is inherently DNA damage tolerant. *Science*, *334*, 235–238.

Yeeles, J. T. P., Poli, J., Marians, K. J., & Pasero, P. (2013). Rescuing stalled or damaged replication forks. *Cold Spring Harbor Perspectives in Biology*, *5*, 1–15.

Zeman, M. K., & Cimprich, K. A. (2014). Causes and consequences of replication stress. *Nature Cell Biology*, *16*, 2–9.